Supplementary material

Green Energy Storage: Upcycling of Lithium-ion Battery for its Utilization in a High-Performance Asymmetric Supercapacitor Device

Umang Singh,[a] Ritika Sharma,[b] Dilbag Singh,[a*] Deepak Pant[a*]

[a] School of Earth and Environmental Sciences, Central University of Himachal Pradesh, Dharamshala, Kangra, Himachal Pradesh-176215
[b] University Research Department, Rayat Bahra University, Mohali, 140103, Punjab, India

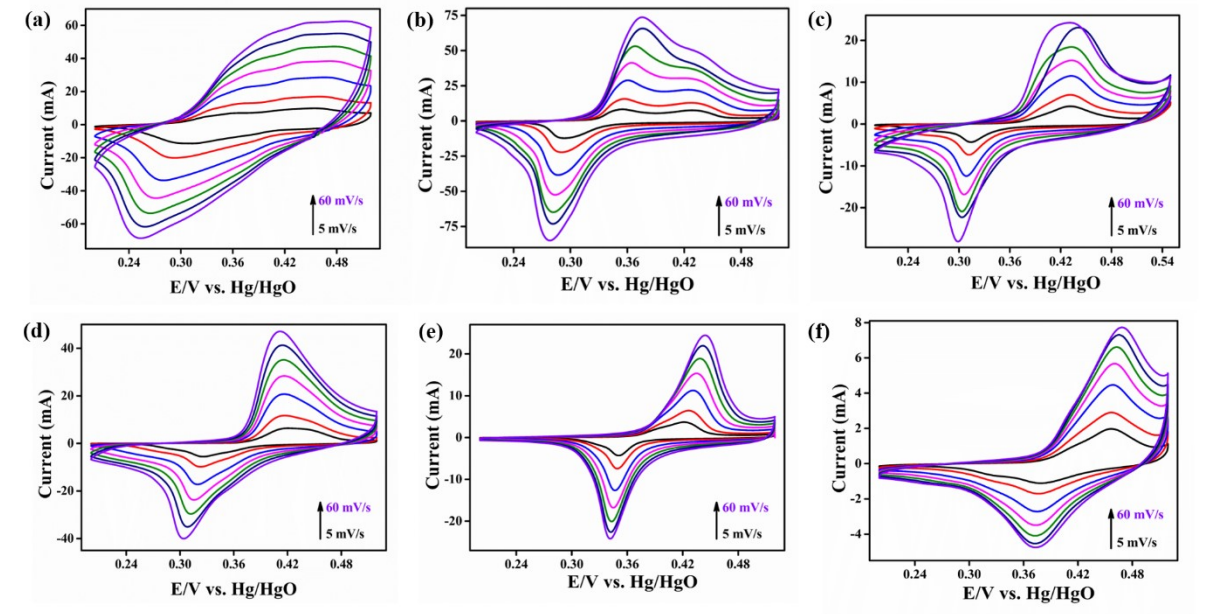

Figure S1 CV at increasing scan rate of (a) LCO-BS_NF; (b) LCO-S_NF; (c) LCO-C_NF; (d) GR-C_NF; (e) GR-S_NF; (f) GR-BS_NF

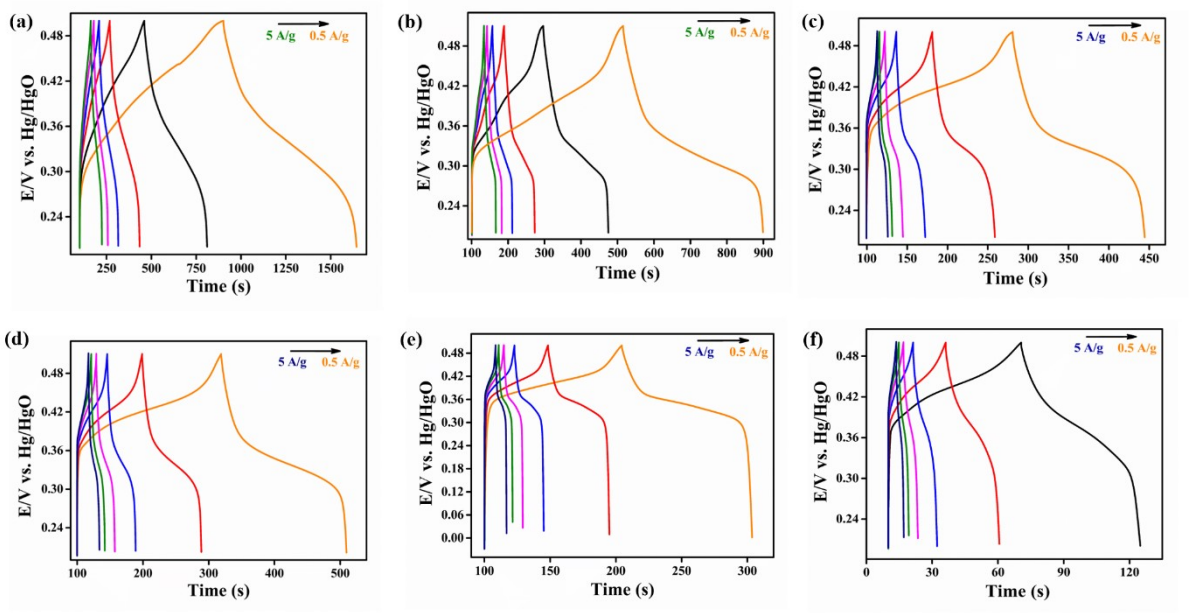

Figure S2 GCD at increasing current density of (a) LCO-BS_NF; (b) LCO-S_NF; (c) LCO-C_NF; (d) GR-C_NF; (e) GR-S_NF; (f) GR-BS_NF

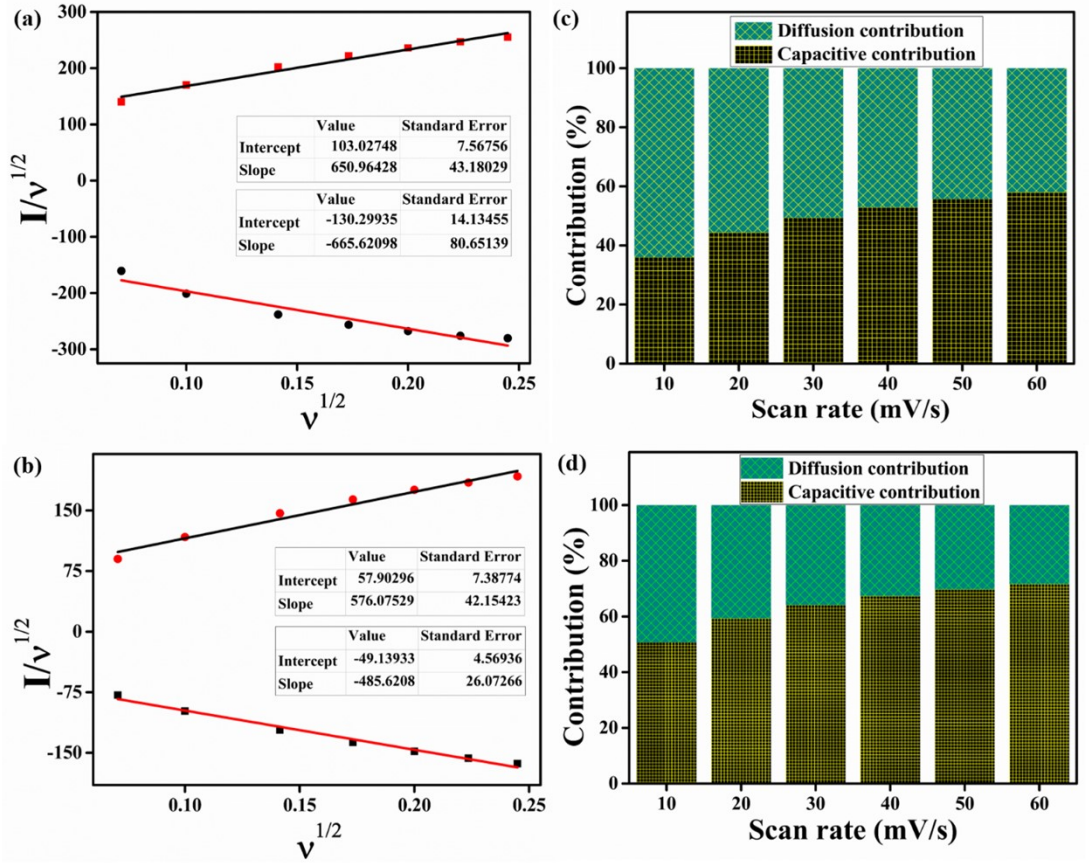

Figure S3 I/ $\upsilon^{1/2}$ versus $\upsilon^{1/2}$ plot for oxidation and reduction current peak of **(a)** LCO-BS_NF and **(b)** GR-C_NF, and relative capacitive and diffusion contribution graphs of **(c)** LCO-BS_NF and **(d)** GR-C_NF.

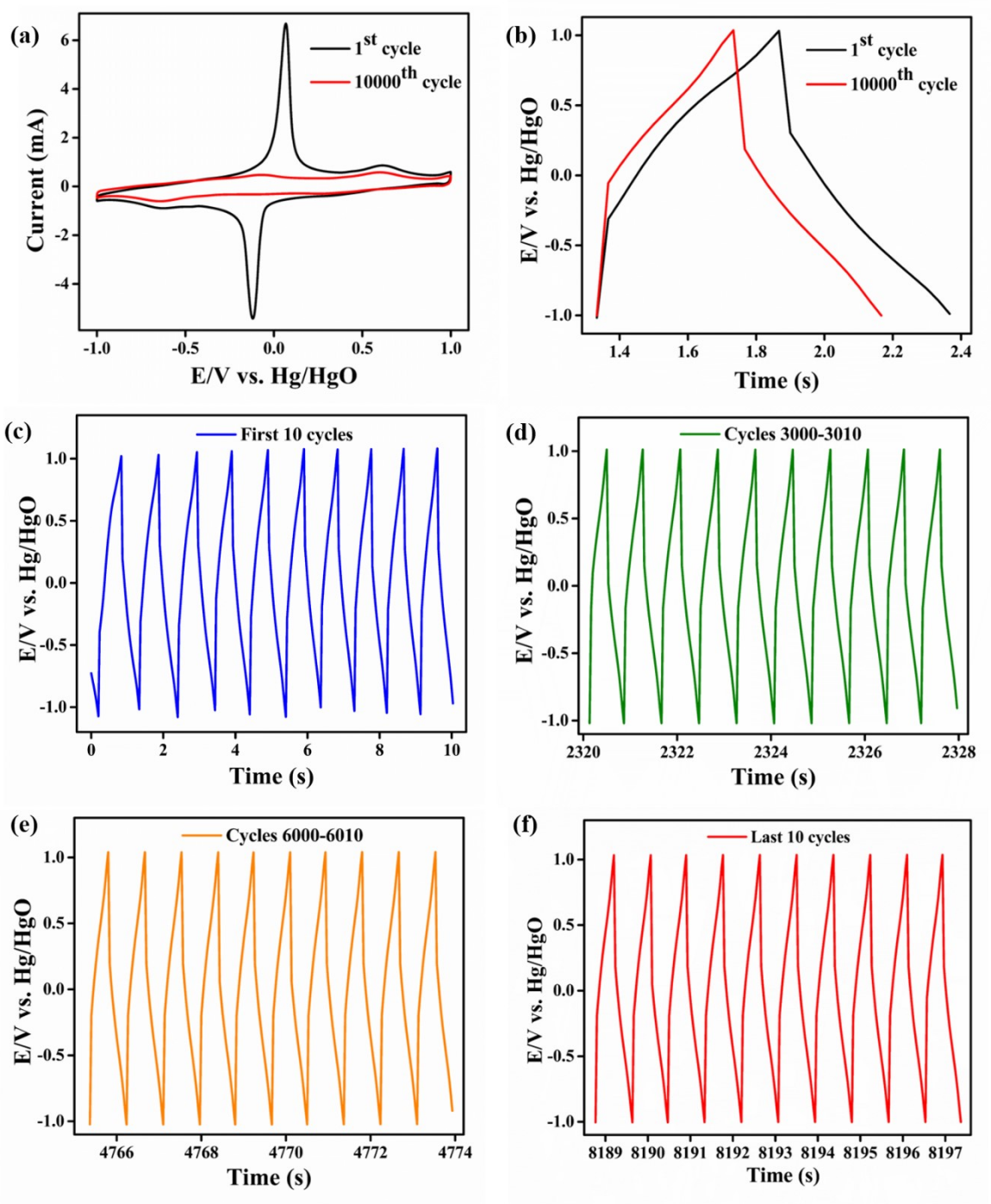

Figure S4 (a) Comparison of CV curve before and after cyclic stability; (b) GCD curve of the first cycle and the last cycle after cyclic stability; (c) first ten cycles of cyclic stability; (d),(e) intermediate cycles of cyclic stability, and (f) last ten cycles of cyclic stability

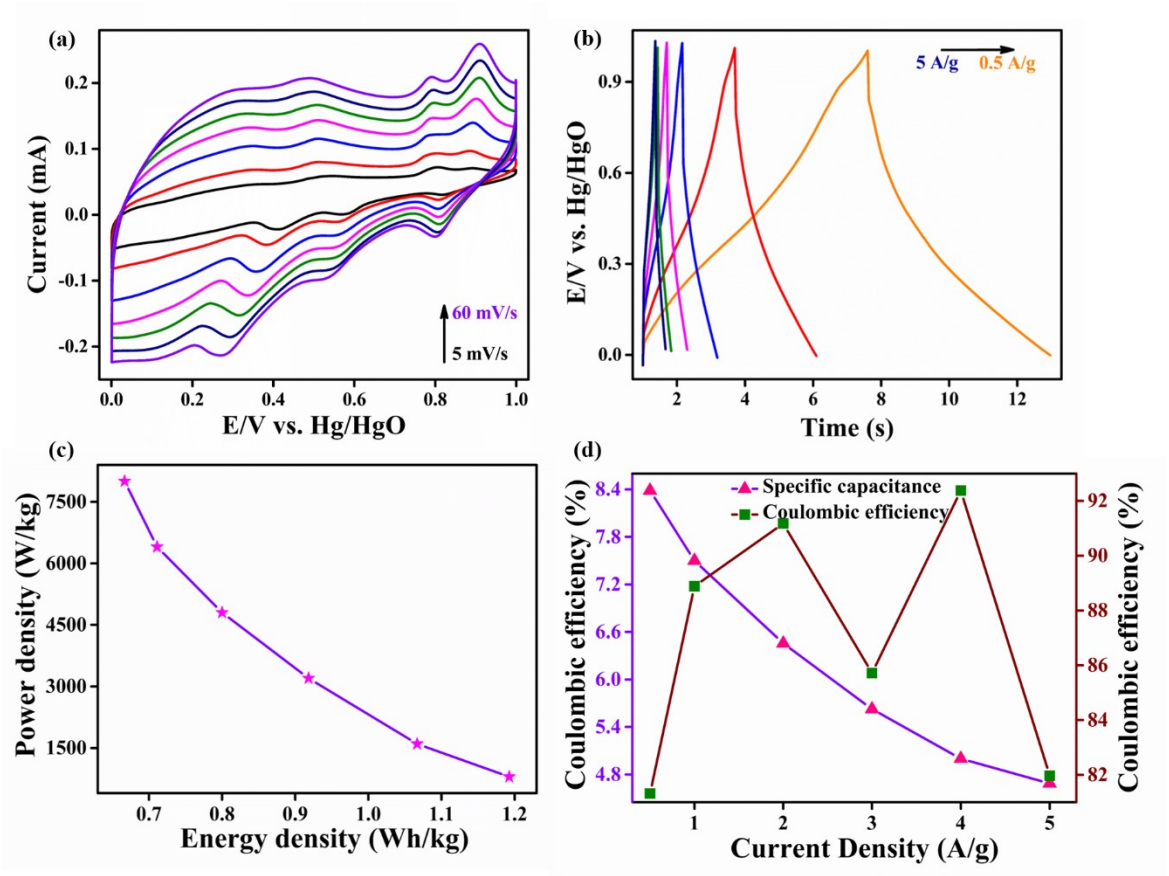

Figure S5 Symmetric device of LCO-BS_NF (a) CV at increasing scan rate; (b) GCD at increasing current density; (c) power density vs energy density curve and (d) graph showing specific capacitance and coulombic efficiency at various current densities

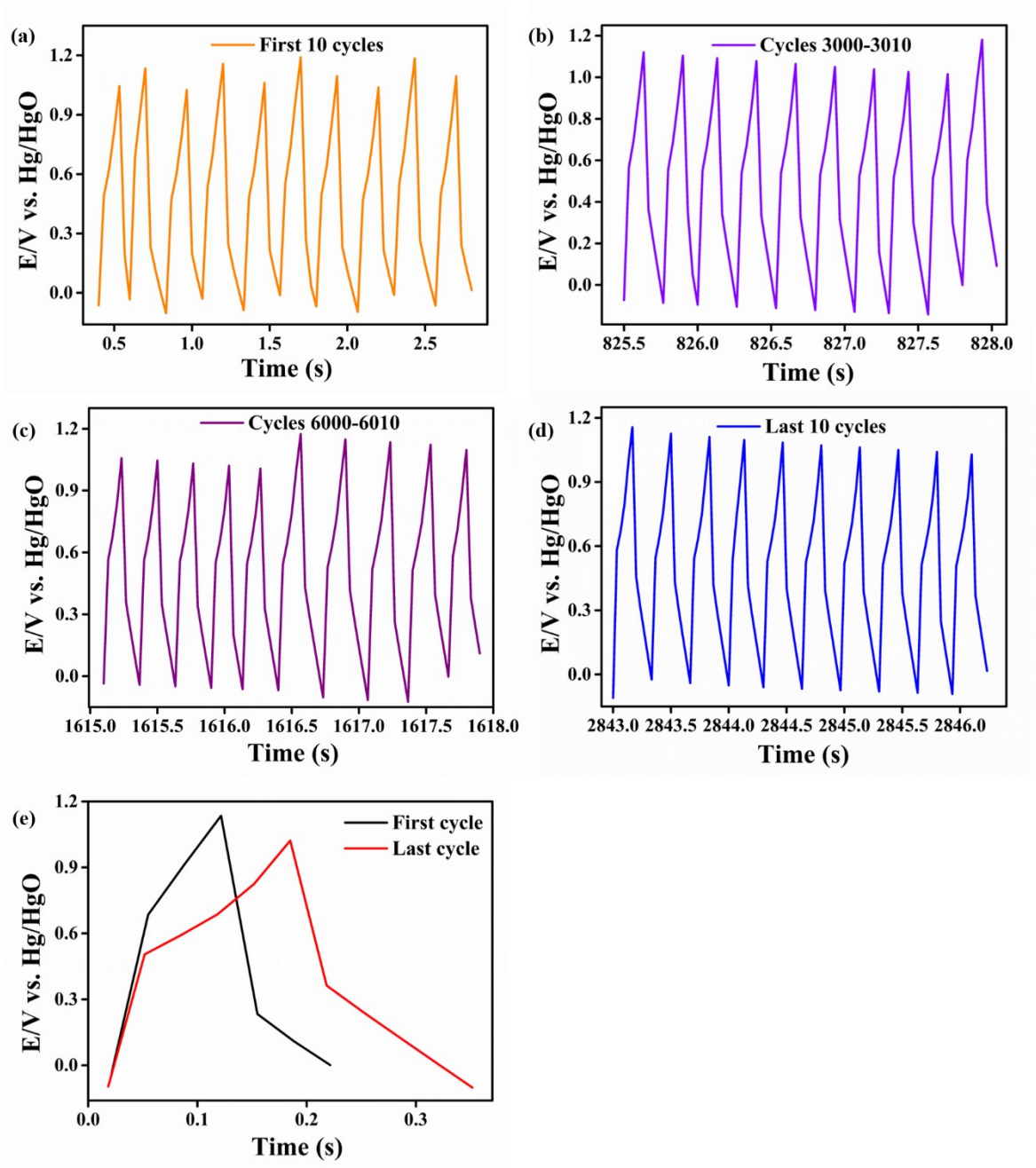

Figure S6 Symmetric device of LCO-BS_NF (a) first ten cycles of cyclic stability; (b),(c) intermediate cycles of cyclic stability; (d) last ten cycles of cyclic stability and (e) GCD curve of the first cycle and the last cycle after cyclic stability

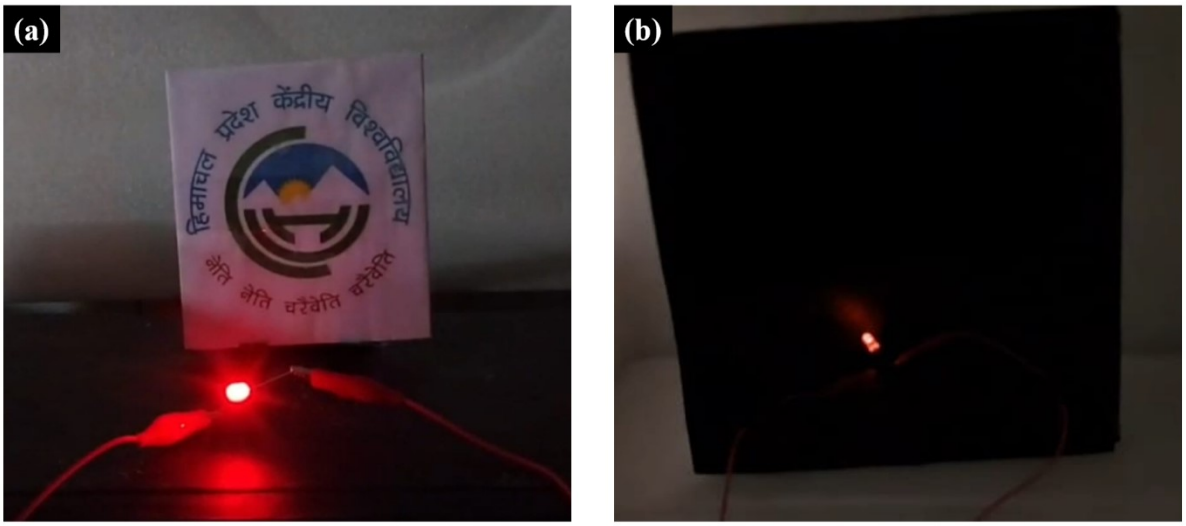

Figure S7 Illumination of red LED bulb by (a) symmetric LCO-BS_NF device and (b) asymmetric LCO-BS_NF and GR-C_NF device

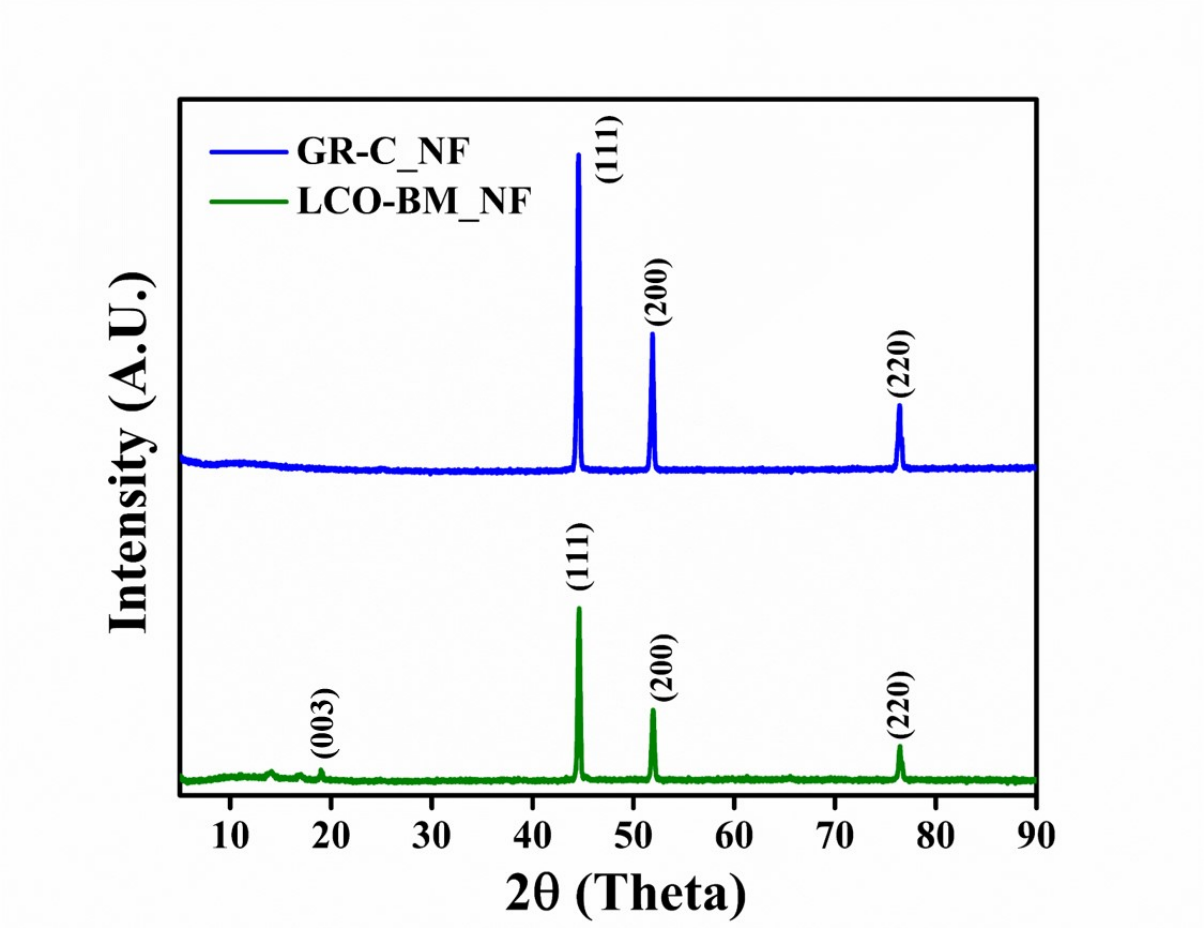

Figure S8 XRD diffractograms of GR-C_NF and LCO-BM_NF

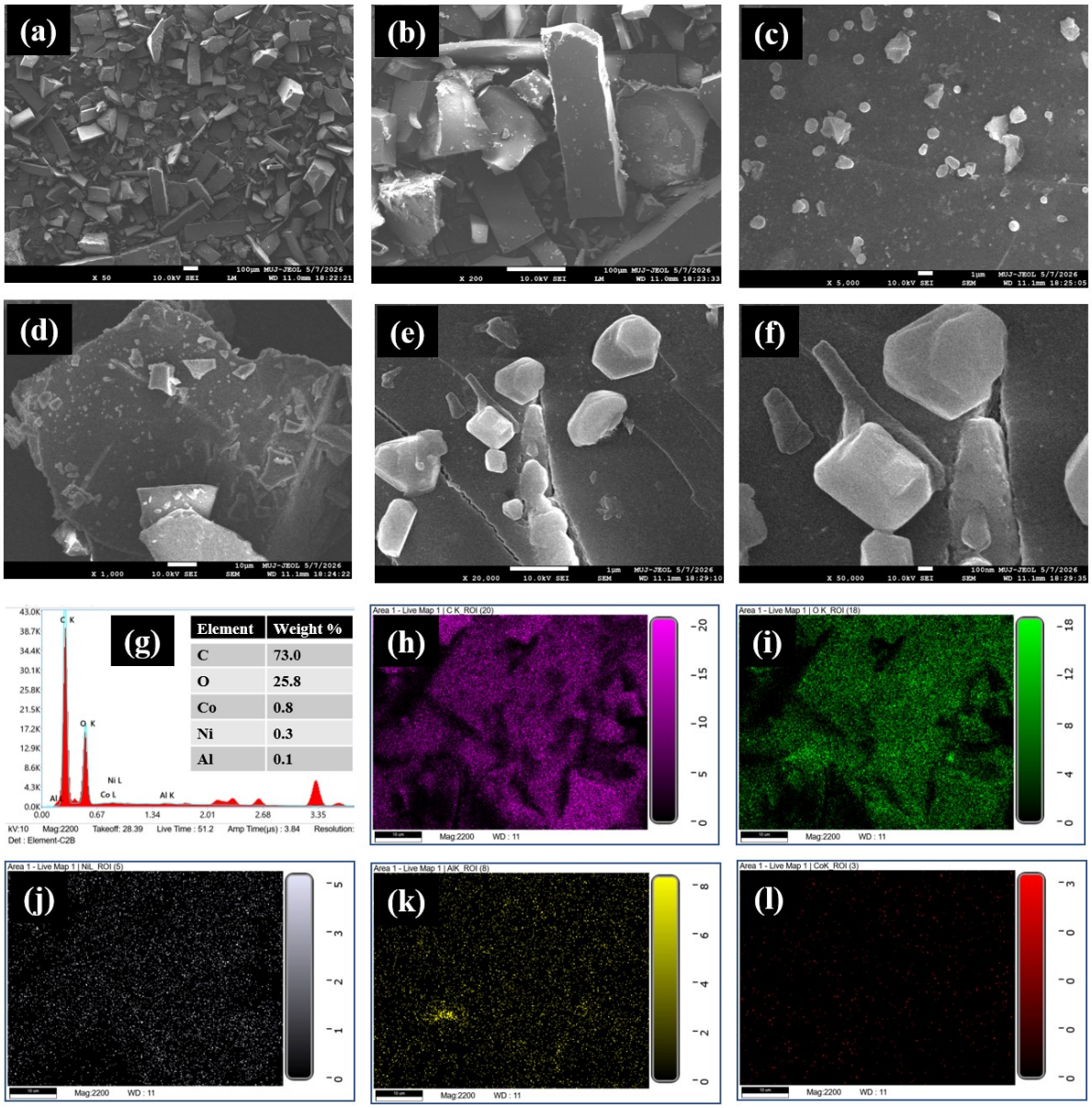

Figure S9 SEM characterization of LCO-C (a-f) SEM micrographs at different magnifications; (g) EDX spectrum and (h-l) elemental mapping of C, O, Ni, Al and Co respectively

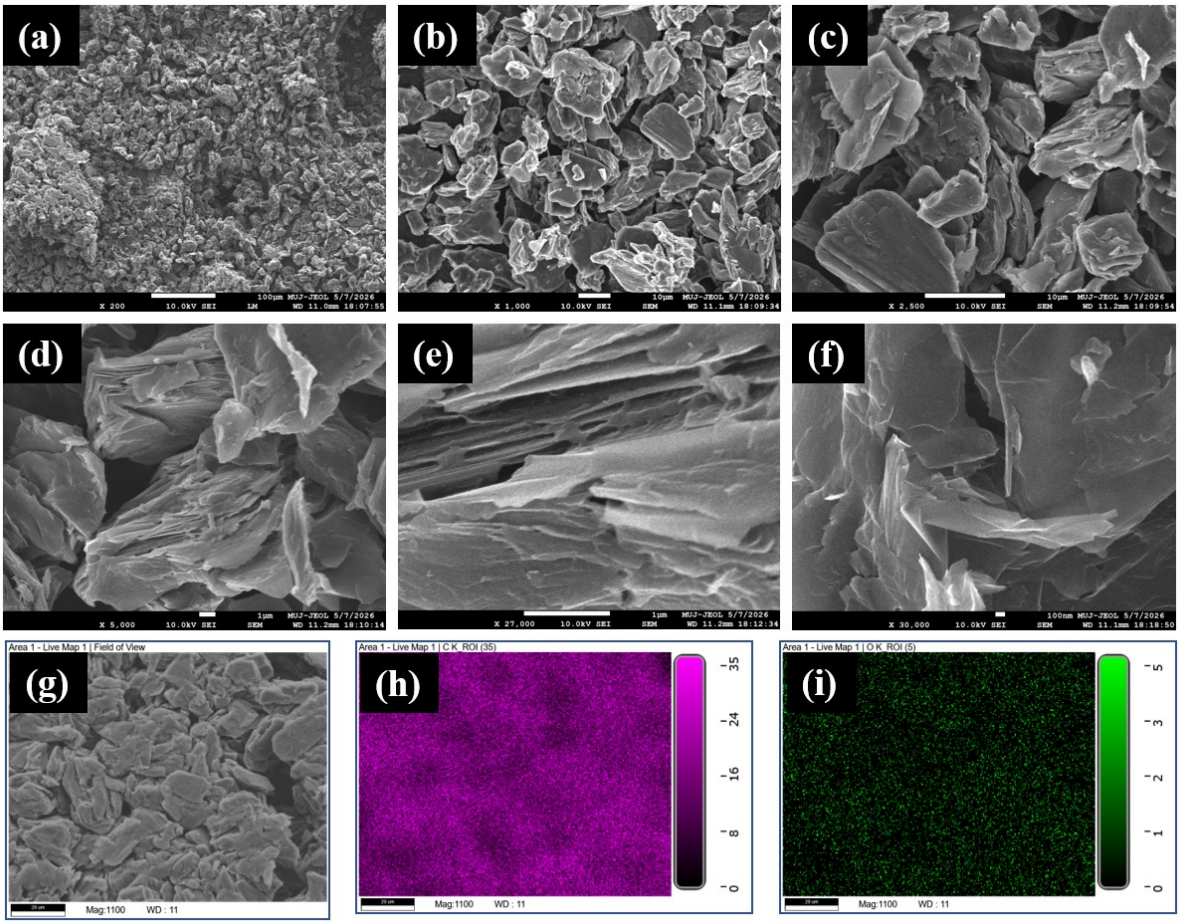

Figure S10 SEM characterization of GR-C (a-g) SEM micrographs at different magnifications and (h,i) elemental mapping of C and O respectively

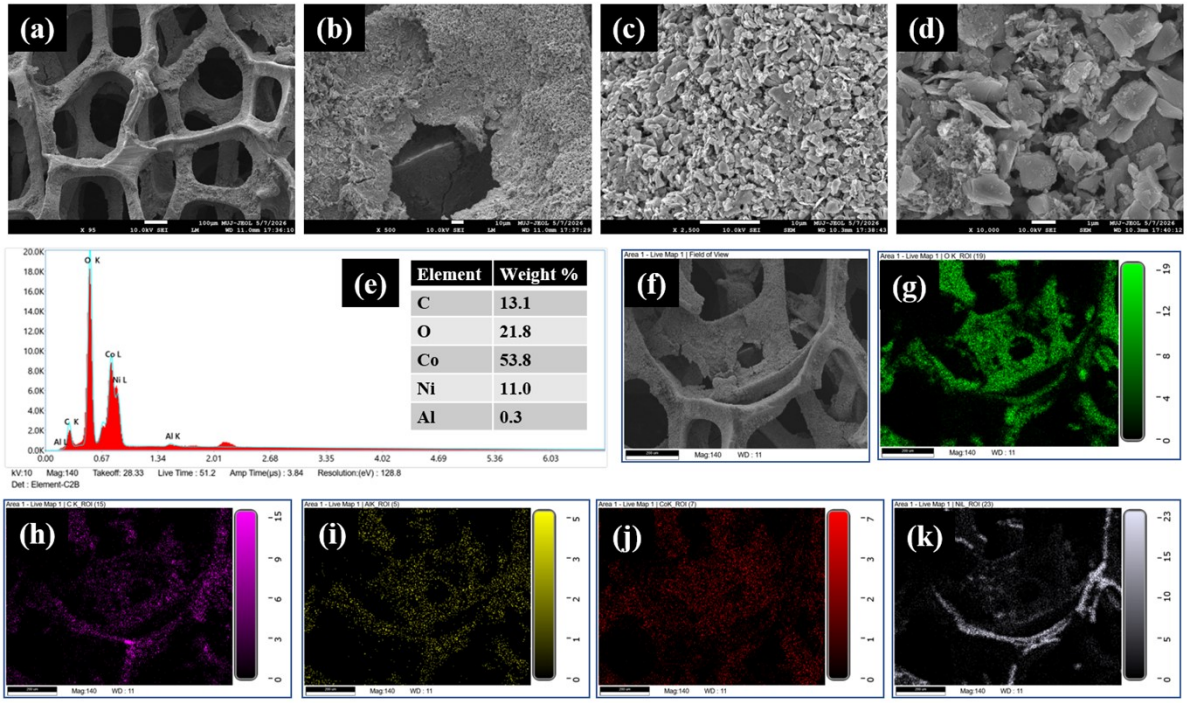

Figure S11 SEM characterization of LCO-BM_NF (a-d) SEM micrographs at different magnifications; (e) EDX spectrum; (f) SEM image selected for elemental mapping and (g-k) corresponding elemental mapping of O, C, Al, Co and Ni respectively

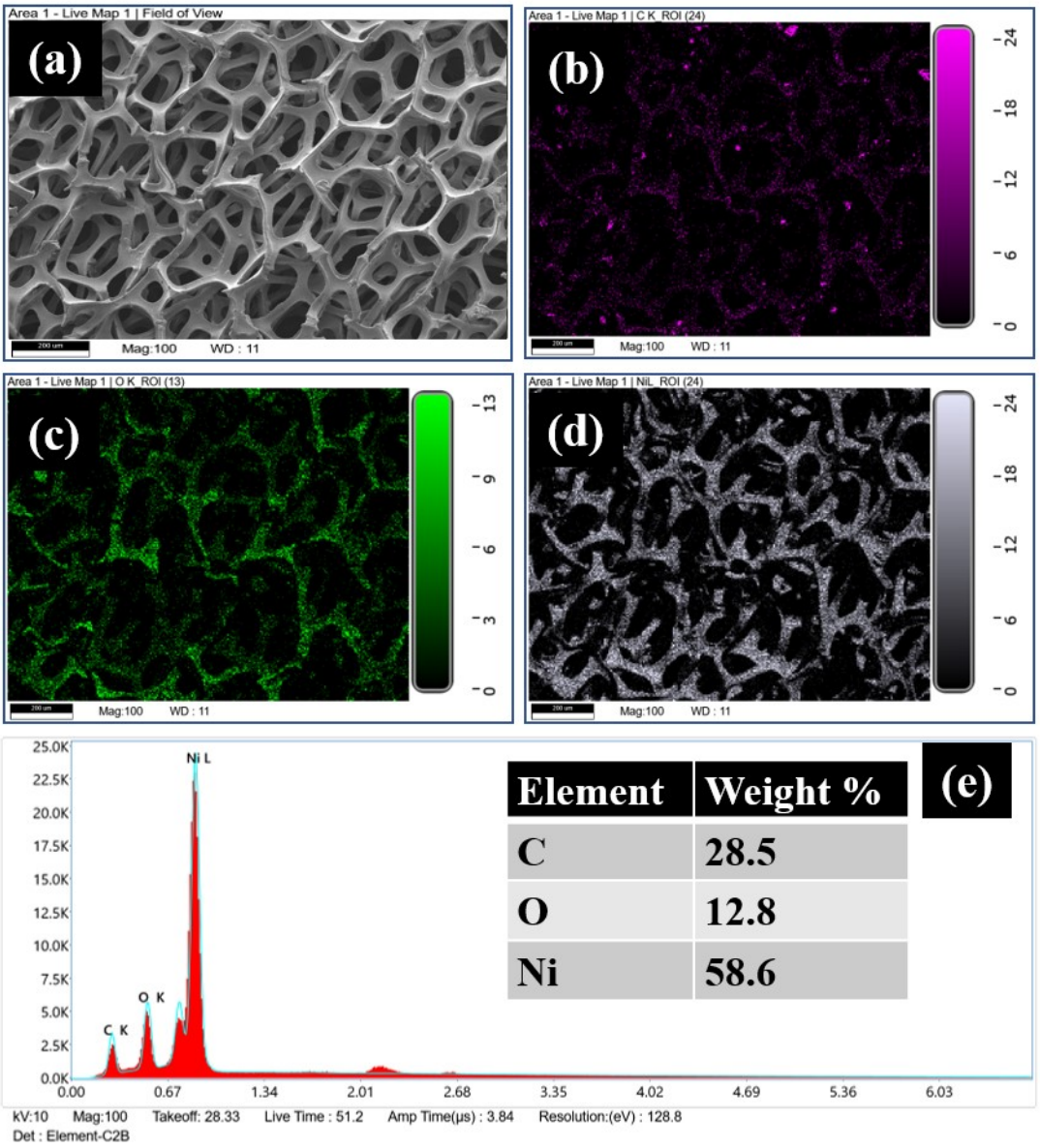

Figure S12 SEM characterization of GR-C_NF (a) SEM image selected for elemental mapping; (b-d) elemental mapping of C, O and Ni respectively and (g) EDX spectrum

Table S1: Literature survey of electrode materials recovered from spent LIBs for SC development

Electrode	Material recovered	Recovery Method	Electrode Synthesis Methods	Specific Capacitance (F/g)	Cyclic stability (%)	Energy density (Wh/kg)	Power density (W/kg)	Ref.
Co_3O_4-450	Cathode	Leaching	Calcination	98 mF/cm^2	100 (1000 cycles)	0.022 mWh/cm^2	0.84 mW/cm^2	[16]
LIB cathode + 10 % CNT	Cathode	Calcination	Doping	165	92 (1000 cycles)	33.4	3239	[18]
Co_3O_4	Cathode	Leaching	Electrodeposition	1273	96 (5000 cycles)	-	-	[17]
CNMOH	Cathode	Leaching	-	1219 mF/cm^2	100 (10,000 cycles)	8.78	263.09	[19]
Li−Ni−Mn−	Cathode	Leaching	Electrodeposition	951	90 (10,000 cycles)	30	377	[20]

Co hydroxides								
TRGNs−MoS_2	Anode	-	Thermal reduction	415	88 (5000 cycles)	14.42	103.86	[21]
GO+GQD	Anode	-	Chemical method	2519	88 (1000 cycles)	126	-	[22]
Graphite@MnO_x	Black mass	Leaching	Chemical method	270	80 (5000 cycles)	0.85	1900	[23]

Table S2: Electrochemical performance parameters of synthesized electrodes

Electrode	Oxidation peak (V)	Current (mA)	CV-derived specific capacitance (F/g)	GCD-derived specific capacitance (F/g)
LCO-S_NF	0.37	65.73	826.46	557.59
LCO-BS_NF	0.48	55.20	1089.61	1167
LCO-C_NF	0.44	23.06	174.63	152.94
GR-C_NF	0.41	41.28	433.07	281.56
GR-S_NF	0.44	21.94	174.63	146.25
GR-BS_NF	0.46	7.31	73.61	82.11

Table S3: Comparison of LCO-BM_NF asymmetric with GR-C_NF with some reported Co-based two-electrode asymmetric systems

Material	Specific capacitance (F/g)	Electrolyte used	Potential window (V)	Energy density (Wh/kg)	Power density (W/kg)	Cyclic stability (%)	Reference
$Co(OH)_2$||PC	260 at 2 A/g	3 M KOH	1.5	76.7	1416.9	91 (5000 cycles)	[57]
$Co_2Mn_3O_8$||HBFC	-	2 M KOH	1.7	24.3	850	91.7 (10,000 cycles)	[58]
NiCuCoO||AC	105 at 1A/g	3 M KOH	1.6	96	841	95 (5000 cycles)	[59]
Co_3O_4–CQD||AC	51 at 0.5 A/g	1 M KOH	1.4	13.88	684.65	96 (5000 cycles)	[60]
$Co(OH)_2$@PANI||AC	385 at 1 A/g	6 M KOH	1.4	31.2	1050	74.8 (5000 cycles)	[61]
MnS/Ni_3S_2@$Co(OH)_2$||AC	219.5 1 A/g	1 M KOH	1.5	68.6	750	91.2 (10,000 cycles)	[62]
Fe–$CoWO_4$||AC	82.6 at 1 A/g	3 M KOH	1.5	25.8	750	77.3 (10,000 cycles)	[63]
CoPO||AC	-	2 M H_2SO_4	1.4	24.02	299.21	99 (5000 cycles)	[64]
$CoMn_4$||AC	81.8 at 0.25 A/g	6 M KOH+PVA	1.6	29.1	320	96.5 (10,000 cycles)	[65]
LCO-BM_NF||GR-C_NF	16.35 at 0.5 A/g	6 M KOH	2	90.87	5,000	53 (10,000 cycles)	Current work